Copyright 2000 by the Society of Photo-Optical Instrumentation Engineers.

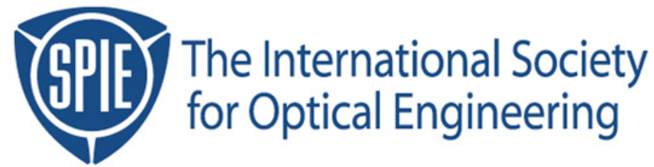

This paper was published in the proceedings of
Photomask and X-Ray Mask Technology VII
SPIE Vol. 4066, pp. 172-179.
It is made available as an electronic reprint with permission of SPIE.

One print or electronic copy may be made for personal use only. Systematic or multiple reproduction, distribution to multiple locations via electronic or other means, duplication of any material in this paper for a fee or for commercial purposes, or modification of the content of the paper are prohibited.

Lithography Performance of Contact Holes — Part II: Simulation of the Effects of Reticle Corner Rounding on Wafer Print Performance

Chris A. Mack, Charles Sauer*, Suzanne Weaver*, and Jan Chabala*

FINLE Technologies, A Division of KLA-Tencor
8834 N. Capital of Texas Highway, Suite 301, Austin, TX 78759 USA
Phone: (512) 327-3781; fax: (512) 327-1510; e-mail: chris_mack@finle.com

*Etec Systems, An Applied Materials Company
26460 Corporate Avenue, Hayward, CA 94545 USA
Phone: (510) 784-7258; fax: (510) 887-2870; e-mail: csauer@etec.com

ABSTRACT

Pattern fidelity of contact features on the wafer is critical to the functionality of a device. Without good pattern fidelity of these features, interconnects between conductor layers may be unreliable, ultimately causing the device to fail. Among other error sources, the feature quality on the reticle is thought to be a key contributing factor to wafer contact pattern fidelity. In particular, the pattern generation tool used to expose the reticle may be selected based on the maximum acceptable amount of corner rounding of a contact feature. Of course, optimization of contact layers is dependent on the exposure and process of both the mask and wafer, as well as on their relationship to one another. Understanding how reticle pattern fidelity affects the patterned image on the wafer helps to optimize both imaging processes.

This paper examines the key parameters that contribute to wafer contact hole pattern fidelity through simulation. The impact of reticle corner rounding on the printed wafer results will be examined for conventional and attenuated phase shifting masks, dense and isolated contacts. Results from this work will be used to predict the acceptable amount of corner rounding on the reticle, and to define a proper metric of reticle shape.

Keywords: Lithography simulation, PROLITH/3D, contact holes

1. Introduction

In wafer lithography it is convenient to assume that the reticle is an ideal representation of the design data and that corner rounding of the final printed wafer pattern is due only to the diffraction limitations of the imaging and other processing effects such as PEB diffusion. In reality, however, the reticle itself suffers from corner rounding which must, to some lesser or greater degree, affect the printed wafer results as well. How does reticle corner rounding contribute to loss of wafer pattern fidelity? How much reticle corner rounding is acceptable? Does reticle corner rounding affect the focus-exposure process window of the wafer patterns? These are important questions to answer considering the cost trade-offs associated with printing reticles with less corner rounding [1].

Since firmly establishing the implications of mask corner rounding for all pattern types and sizes is a daunting task, a first step is to consider the simplest of cornered mask features, the contact hole. It is well known that when contact hole wafer dimensions are less than about $1.0\lambda/NA$ (where λ is the imaging wavelength and NA is the objective lens numerical aperture), the nominally square holes print as circles on the wafer due to the diffraction limits of the imaging tool [2]. It seems logic that, in this common and important case, the *shape* of the

printed wafer results is not directly affected by the amount of corner rounding on the mask. It is not clear, however, how mask pattern shape affects the size and process window of the wafer patterns.

This paper examines the key parameters that contribute to wafer contact hole pattern fidelity through simulation. The impact of reticle corner rounding on the printed wafer patterns will be examined for conventional and attenuated phase shifting masks (PSM), dense and isolated contacts. Results from this work will be used to predict the acceptable amount of corner rounding on the reticle, and to define the proper metric of reticle shape.

2. Theory

For small contact holes, the aerial image projected by the imaging tool is governed essentially by the point spread function (PSF) of the tool. Defined as the image of an isolated, infinitely small pinhole on the mask, the PSF determines the smallest contact hole that could be printed with conventional imaging. For an ideal, diffraction limited imaging tool, the width of the PSF is about $0.66\lambda/NA$ [3]. Thus, contact holes on the mask with sizes less than this value will not print smaller than the PSF, but will be limited by the PSF width. In fact for contact holes near this limit, the main impact of changing reticle size is simply a reduction of the peak intensity of the contact hole image, which will be proportional to the area of the reticle contact.

With the above description in mind, if two small contact holes have different shapes but the same area, it seems likely that they would produce similar aerial images. To test this idea, consider the two extremes of contact hole corner rounding, a square and a circle. The area of the two are kept constant by making the width of the circle equal to $\sqrt{4/\pi}$ times the width of the square. As a common and important example, consider a nominal 150nm contact hole (wafer dimensions) imaged by a 0.7 NA, 248nm imaging tool (making $k_1 = 0.423$). We can begin by simply examining the diffraction patterns of the square and circular contact holes. The square will produce a diffraction pattern that is the product of two sinc functions, while the circle will produce a Bessel diffraction pattern (Figure 1). Examining a horizontal cross-section of the diffraction patterns in more detail (Figure 2), one can see that the central portions of the two diffraction patterns are nearly identical. The differences lie mostly in the high spatial frequency region.

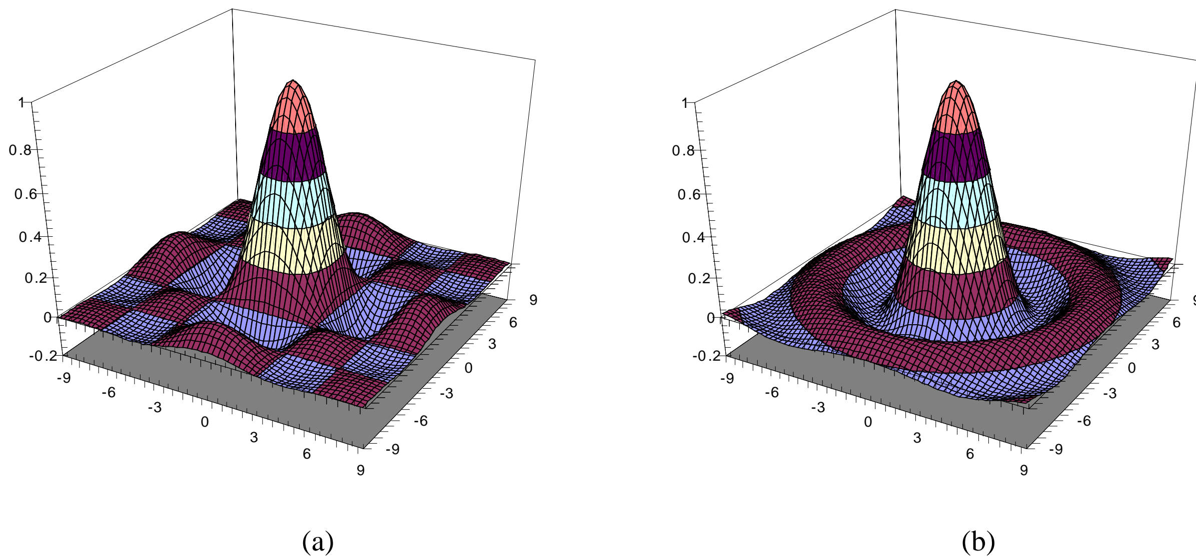

Figure 1. Diffraction patterns for (a) a square contact hole mask pattern, and (b) a circular contact hole mask pattern.

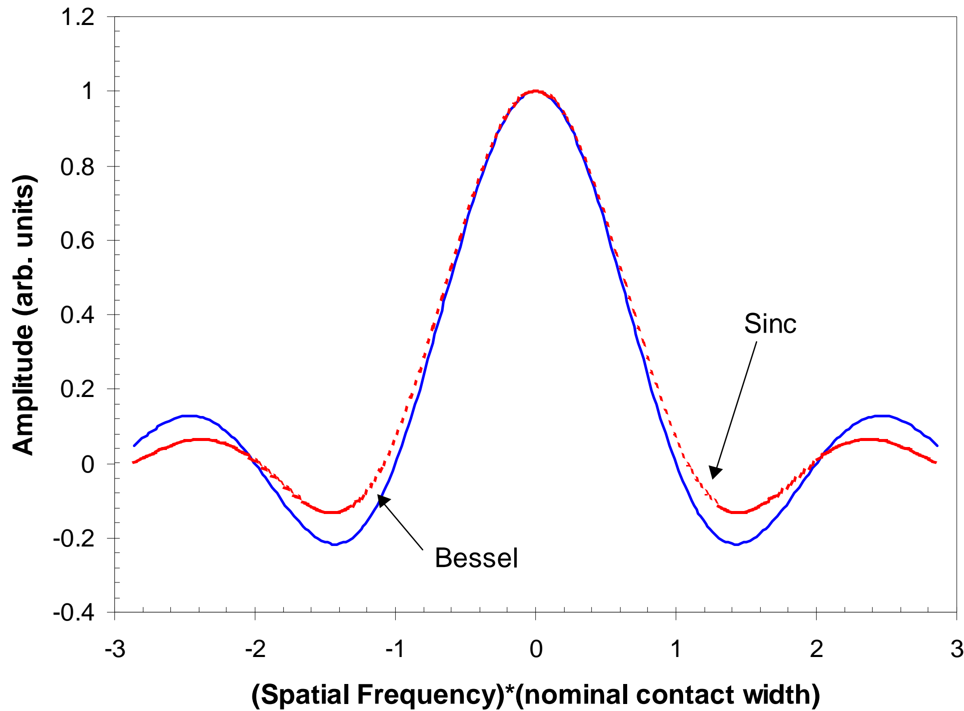

Figure 2. Comparison of horizontal cross-sections of the Bessel (circular mask) and the sinc (square mask) diffraction patterns.

The diffraction patterns of Figures 1 and 2 pass through the low pass filter of the objective lens, cutting off all spatial frequencies greater than NA/λ and less than $-NA/\lambda$. The product of this spatial frequency cut-off and the nominal contact hole width is k_1. Thus, for the example given here with $k_1 = 0.423$, the cut-off of Figure 2 occurs at ±0.423. One can see that in this narrow region of low spatial frequencies the two diffraction patterns are nearly identical. Thus, one would also expect the resulting aerial images to be nearly identical as well.

3. Aerial Image Simulations

Aerial image simulations were performed using PROLITH/3D v6.1 using the High NA Scalar model [4] and λ = 248nm, NA = 0.7, no aberrations or flare, σ = 0.4 or 0.7, and 4X reduction. All mask contact hole patterns were adjusted to have an area of 150X150nm, with corner rounding varying from a corner rounding radius of 0 (square mask) to 84.6nm (circular mask). Pitch was varied from dense (300nm), to semi-dense (450nm) to isolated (1500nm). For the attenuated PSM case, the background intensity transmittance was 6% and only the semi-dense pitch was examined.

Figure 3 shows a representative aerial image result. As a function of reticle corner rounding radius the resulting aerial images varied only slightly. In fact, the only variation was in the value of the peak intensity at the center of the contact hole. Figure 4 shows the peak intensity as a function of corner radius, with a total variation of only 1.4%. In fact, all of the cases studied showed identical trends where the only perceptible change in the aerial image was an increase in the peak intensity as a function of corner rounding. The worst case range of intensities was 2.3% (for both the dense contact and the semi-dense attenuated PSM contact). Although there was no perceptible change in the widths of the aerial images as a function of corner rounding, this small change in peak intensity has some impact in the final printed results.

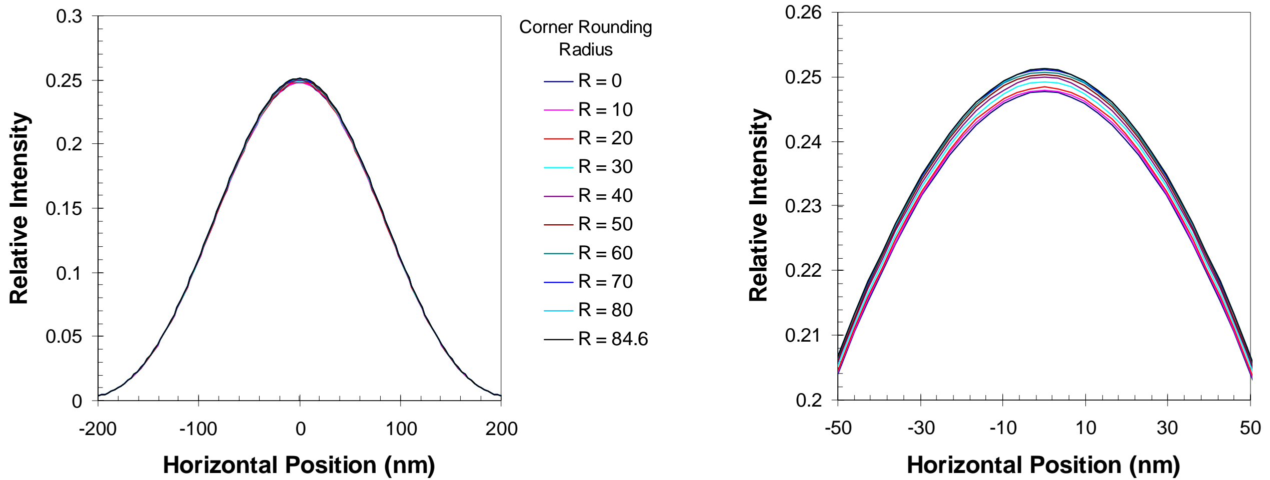

Figure 3. Aerial image results as a function of corner rounding radius (σ = 0.4, isolated binary contacts) shown at two different graph scales.

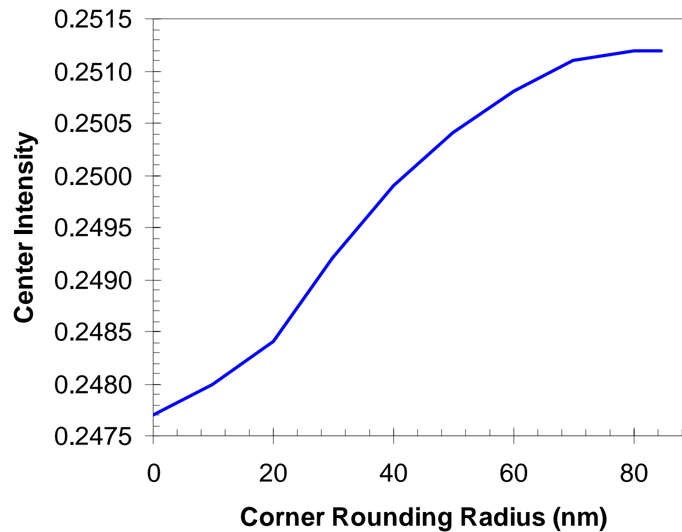

Figure 4. Variation of the peak intensity of the aerial images of Figure 3 as a function of corner rounding shows only a 1.4% change.

4. Resist Simulation Results

Three-dimensional resist simulations were carried out using the conditions given above and using 410nm of UV6 resist on 60nm of AR2 on silicon and with a 125°C, 60 second post exposure bake. A typical example (σ = 0.4, isolated binary contacts) comparing square and completely circular contacts is shown in Figure 5. There is no perceptible difference in resist profile shape and only a slight difference in resist contact width. Figure 6 shows how the critical dimension of the contact hole varies with the amount of corner rounding. Interestingly, the

1.4% variation in aerial image peak intensity leads to a 2.5% variation in resulting CD, showing the importance of the image center intensity in determining linewidth.

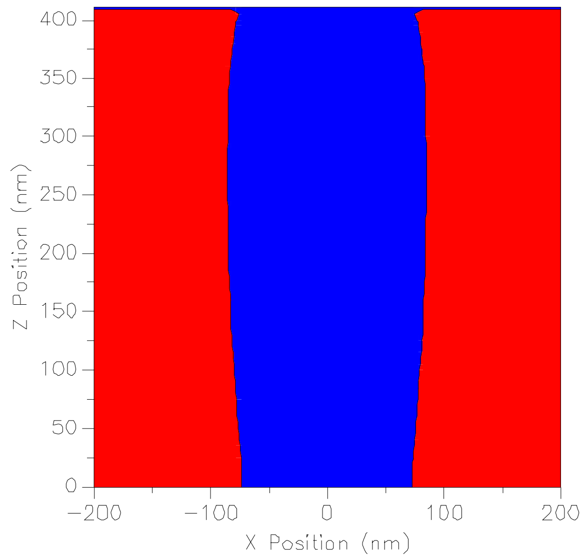

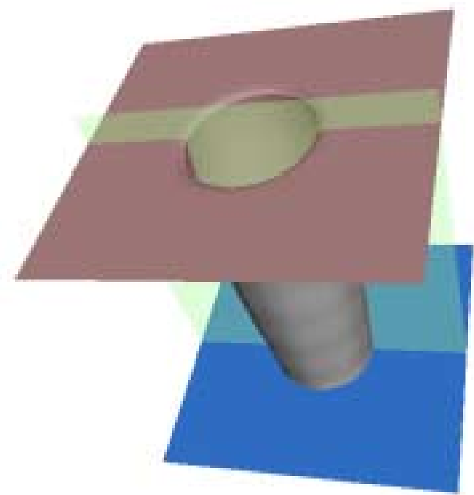

(a)

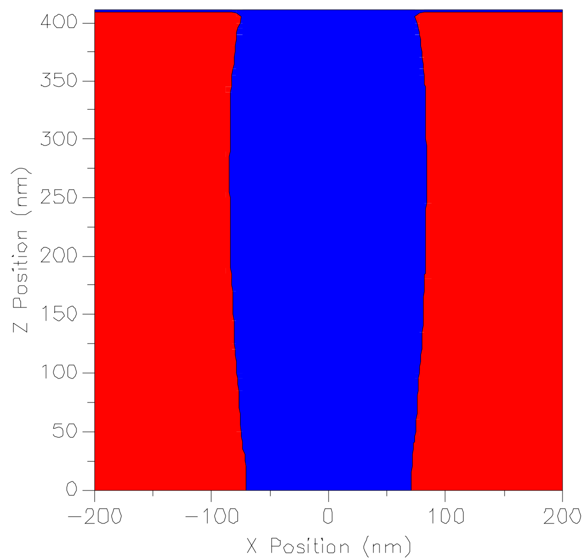

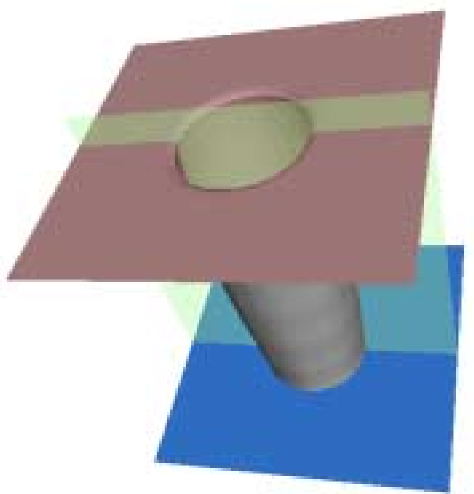

(b)

Figure 5. Resist profile simulations for (a) a square mask, and (b) a perfectly circular mask, both with the same contact hole area on the mask.

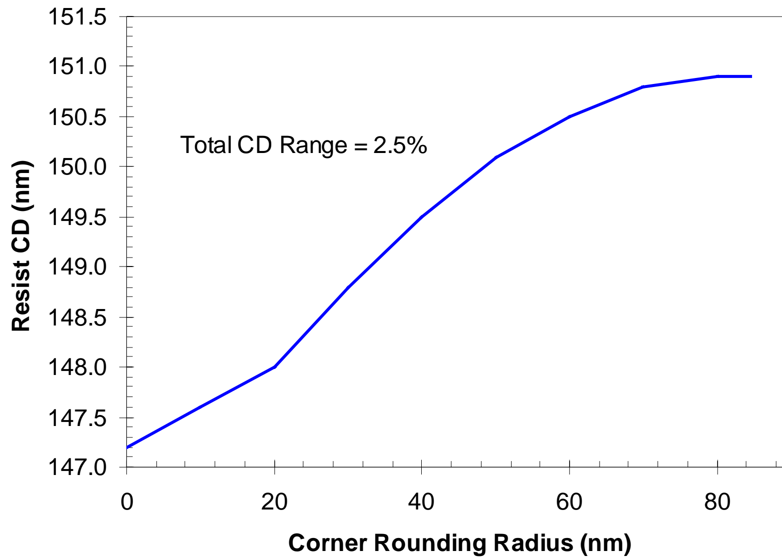

Figure 6. Variation of the resist contact hole CD for the aerial images of Figure 3 as a function of corner rounding shows a 2.5% change.

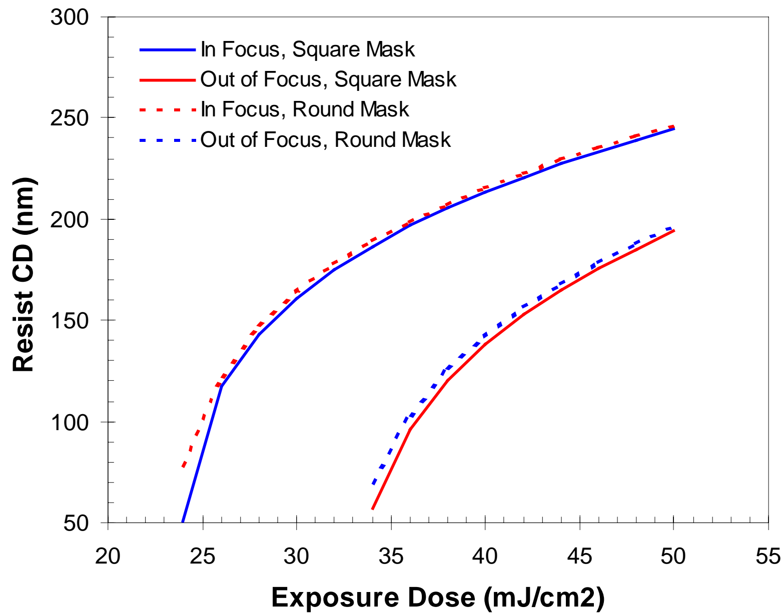

Figure 7. The process response (exposure latitude in and out of focus) of the contact holes for both square and round mask patterns shows that mask corner rounding for these features does not significantly affect the size of the contact hole process window.

Of course, the effects of mask corner rounding on the printability of the pattern in resist at nominal dose and focus tells only a part of the story. Figure 7 shows exposure latitude (CD through exposure) both in and out of focus for the same square and round mask patterns as the previous figures. Other than the 2.5% offset in contact width, the process responses of the two mask patterns are nearly identical. Thus, mask corner rounding seems to have no affect on the size of the process window for these features.

5. Results and Conclusions

In this paper, the impact of mask corner rounding on the wafer printing results was examined for a specific high resolution contact hole pattern: 150nm contacts printed at 248nm with NA = 0.7. The pitch of the contacts was varied between dense and isolated, the partial coherence was changed from moderately low (0.4) to moderately high (0.7), and semi-dense attenuated PSM contacts were also examined. For each contact hole type, the amount of mask corner rounding was varied between a perfectly square contact and a perfectly circular contact, being sure to *keep the area of each mask pattern equal*. All contact mask patterns were studied using simulation to predict the printed wafer results.

Aerial image simulation results show that mask corner rounding produces only a slight variation in the shape of the aerial image. Rounder contacts are slightly brighter than squarer contacts of the same area. Clearly, the square corners have the effect of diffracting a little more light into higher spatial frequencies, reducing the total energy passing though the objective lens. The impact is reasonably small, with peak intensities of the resulting images varying by only 1.4% to 2.3% over the range of pitches studied. Note that the widths of the aerial images are unaffected by the mask corner rounding.

Resist images show essentially the same behavior as the aerial images. The small variation in aerial image peak intensity results in a somewhat larger variation in final resist CD. The shape and cross-section of the resist images remain unchanged with mask corner rounding. Further, simulations through focus and exposure show that the amount of mask corner rounding has very little effect on the size of the resulting process window.

From these results, one can draw several conclusions. First, although the impact of mask corner rounding radius on final resist CD is small, it is not negligible. If the corner rounding radius on the mask varied by about 20nm across the plate, the results would be a 1% final wafer CD variation for the conditions shown here. Thus, the control of corner rounding uniformity should be considered in the mask making process. Second, the key conclusion is that the impact of mask corner rounding is completely dwarfed by the effect of the area of the contact hole on the mask. The peak intensity of the aerial image of a small contact hole is proportional to the area of the contact hole on the mask ("small" being defined as on the order of or smaller than the width of the point spread function of the imaging tool). To first order, the area of the mask contact hole pattern is the only variable of importance. In fact, we propose that, for small contact holes, the effective mask critical dimension be defined as the square root of the area of the mask pattern:

$$\textit{effective mask contact CD} = \sqrt{\textit{contact hole area}}$$

When printing small contact hole mask patterns, all efforts should focus on controlling the effective mask contact hole CD.

References

1. S. Weaver, M. Lu, J. Chabala, D. Ton, C. Sauer, and C. A. Mack, "Lithography Performance of Contact Holes - Part I. Optimization of Pattern Fidelity Using MPG and MPG-II", these proceedings.

2. C. A. Mack and J. E. Connors, "Fundamental Differences Between Positive and Negative Tone Imaging," *Optical/Laser Microlithography V, Proc.*, SPIE Vol. 1674 (1992) pp. 328-338, and *Microlithography World*, Vol. 1, No. 3 (Jul/Aug 1992) pp. 17-22.

3. C. A. Mack, "The Natural Resolution", *Microlithography World* (Fall, 1998).

4. C. A. Mack, Inside PROLITH: A Comprehensive Guide to Optical Lithography Simulation, FINLE Technologies (Austin, TX: 1997).